Electron spin resonance in a model $S = \frac{1}{2}$ chain antiferromagnet with a uniform Dzyaloshinskii-Moriya interaction

A. I. Smirnov,[1] T. A. Soldatov,[1,2] K. Yu. Povarov,[3,*] M. Hälg,[3] W. E. A. Lorenz,[3] and A. Zheludev[3]
[1]*P. L. Kapitza Institute for Physical Problems, RAS, 119334 Moscow, Russia*[†]
[2]*Moscow Institute for Physics and Technology, 141700 Dolgoprudny, Russia*
[3]*Neutron Scattering and Magnetism, Laboratory for Solid State Physics, ETH Zürich, Switzerland*[‡]
(Received 27 July 2015; revised manuscript received 6 October 2015; published 22 October 2015)

The electron spin resonance spectrum of a quasi-1D $S = 1/2$ antiferromagnet $K_2CuSO_4Br_2$ was found to demonstrate an energy gap and a doublet of resonance lines in a wide temperature range between the Curie-Weiss and Neèl temperatures. This type of magnetic resonance absorption corresponds well to the two-spinon continuum of excitations in $S = 1/2$ antiferromagnetic spin chain with a uniform Dzyaloshinskii-Moriya interaction between the magnetic ions. A resonance mode of paramagnetic defects demonstrating strongly anisotropic behavior due to interaction with spinon excitations in the main matrix is also observed.

DOI: 10.1103/PhysRevB.92.134417 PACS number(s): 75.40.Gb, 76.30.−v, 75.10.Jm

I. INTRODUCTION

One-dimensional $S = 1/2$ antiferromagnets are intensively studied because of the numerous collective quantum effects, including the spin-liquid behavior at zero temperature and fractionalized spin excitations (spinons) [1], revealing itself in a form of two-particle continuum [2,3]. In applied magnetic field this continuum splits into transverse and longitudinal branches and develops a fine structure [4,5]. Typically, this fine structure is undetectable by the electron spin resonance (ESR) experiments probing strictly $q = 0$ excitations. However, some additional perturbations may dramatically modify the long-wavelength response of the spin chain [6]. We address now a fine structure of the two-spinon continuum, appearing at $q = 0$ in spin chains with the so-called uniform Dzyaloshinskii-Moriya (DM) interaction.

A feature of the *uniform* DM interaction is the parallel orientation of characteristic vectors **D** for all bonds within a chain. This pattern is fundamentally different from that of a conventional *staggered* DM interaction, when vectors **D** compose an alternating antiparallel structure. The staggered DM interaction is known to induce a canting of magnetic sublattices in a classical antiferromagnet, resulting in a weak ferromagnetic moment [7,8]. The uniform interaction would stabilize a spiral spin structure in a classical chain. For a quantum spin chain, which has a disordered ground state, a uniform DM interaction modifies the spectrum of excitations [9–11]. In particular, this causes a shift of the spinon continuum in momentum space by a specific wave vector $q_{DM} = D/Ja$ (here J is the exchange integral and a the interspin distance). As a result, in a magnetic field $\mathbf{H} \parallel \mathbf{D}$ the ESR line splits into a doublet. The frequencies of the doublet components are at the upper and lower boundaries of the initial (i.e., unshifted) continuum of transverse spin fluctuations at the wave vector q_{DM} [9,11]. Thus the doublet is marking the width of the continuum at this particular wave vector.

At the same time, the ESR signal should not split at $\mathbf{H} \perp \mathbf{D}$. Another consequence of the spectrum modification is a gap of the ESR absorption in zero field. This case should not be confused with the gapped "breather" mode arising in nonzero field in spin chains with staggered DM, as described in Refs. [6,12]. The described modifications stem from the nonequivalence of spinons, propagating in different directions along the spin chain under the action of uniform DM interaction and they are the consequence of the fractionalized nature of excitations [9,11]. Emerging fine structure enables one, in particular, to measure the width of the continuum of transverse spin oscillations near the origin of the Brillouin zone by means of ESR. The manifestation of the spinon continuum in ESR response was indeed observed in Cs_2CuCl_4—a frustrated $S = 1/2$ quasi-2D distorted triangular lattice antiferromagnet [10,13,14]. The observed 1D behavior in a nominally 2D system was associated with the effective decoupling of spin chains due to the frustration of interchain bonds within the triangular lattice.

Recently, a true spin $S = 1/2$ antiferromagnetic chain compound with uniform Dzyaloshinskii-Moriya interaction $K_2CuSO_4Br_2$ was synthesized and studied by Hälg *et al.* [15]. The structure of this orthorhombic *Pnma* mineral is shown in Fig. 1. The magnetic $S = 1/2$ Cu^{2+} ions are linked by the two-bromine superexchange pathways in chains, running along the a axis. The value of the intrachain exchange integral $J = 20.5$ K is 600 times larger than the interchain exchange J'. Thus the correspondence of this material to the 1D model is much more exact than for the above mentioned Cs_2CuCl_4. Like other low-dimensional magnets, $K_2CuSO_4Br_2$ does not order magnetically at cooling far below the Curie-Weiss temperature. It orders antiferromagnetically at $T_N \simeq 70$ mK, while the Curie-Weiss temperature is about 20 K, thus demonstrating a very good correspondence to 1D model. The model Hamiltonian of a spin chain including Heisenberg exchange and uniform Dzyaloshinskii-Moriya interactions may be written as

$$\mathcal{H} = \sum_i (J\mathbf{S}_i\mathbf{S}_{i+1} + \mathbf{D} \cdot \mathbf{S}_i \times \mathbf{S}_{i+1}). \quad (1)$$

[*]Previous address: P. L. Kapitza Institute for Physical Problems, RAS, 119334 Moscow, Russia.
[†]http://kapitza.ras.ru/rgroups/esrgroup/Welcome.html
[‡]http://www.neutron.ethz.ch/

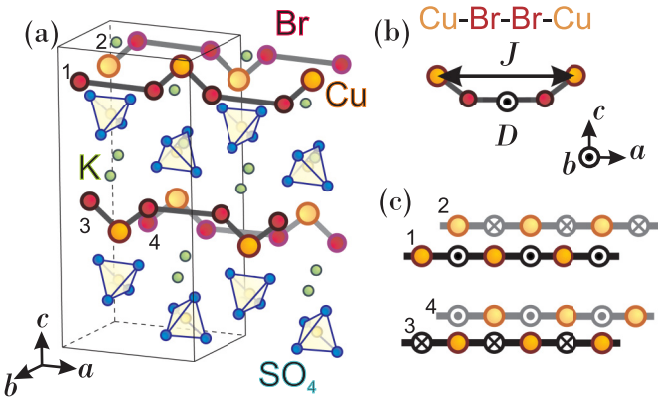

FIG. 1. (Color online) (a) Schematic representation of $K_2CuSO_4Br_2$ crystal structure. (b) Magnetic interactions between the Cu^{2+} ions as given in Hamiltonian (1). Vector **D** presents the symmetry allowed parameter of Dzyaloshinskii-Moriya interaction. (c) Two sets of nonequivalent spin chains with the opposite direction of DM vector.

Here J is the intrachain exchange integral and vector **D** is the parameter of DM interaction. For $K_2CuSO_4Br_2$ the DM vectors in adjacent chains are of the same absolute value but are directed along opposite directions, being parallel to b axis, as shown by the symmetry analysis [15]. This arrangement is simpler than in Cs_2CuCl_4, where a few nonparallel DM vector directions exist in adjacent chains. A comparison of the structures constructed by the DM vectors in both compounds is given in Fig. 2. The simple collinear structure of DM vectors in $K_2CuSO_4Br_2$ enables one to adjust the magnetic field parallel to all DM vectors, which was impossible for Cs_2CuCl_4. This possibility may allow one to observe a specific soft mode in a magnetic field when the Zeeman energy takes a specific value determined by DM energy. The observation of the splitting of the ESR line in $K_2CuSO_4Br_2$ at the frequency $\nu = 26.86$ GHz at cooling below 20 K was briefly reported in Ref. [15]. Now we describe the investigation of the ESR spectrum of this compound in a wide frequency and temperature range. Our measurements cover the subgap and overgap frequency domains, reconstructing the entire frequency-field dependence of ESR absorption. The anisotropy of the effect is also checked to be consistent with the spinon-based theory [9]. Besides, we follow

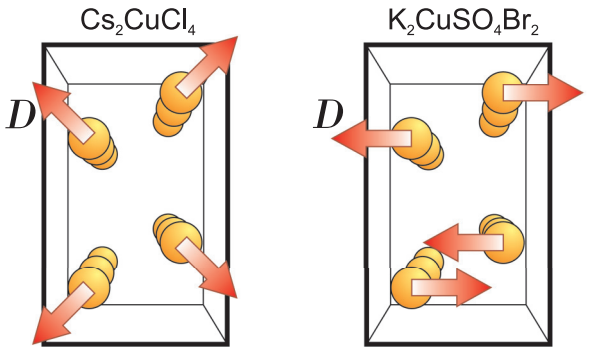

FIG. 2. (Color online) Comparison of the Dzyaloshinskii-Moriya vectors in Cs_2CuCl_4 and $K_2CuSO_4Br_2$. Perspective view along the spin chains.

the temperature dependence of the gap and of the splitting of the doublet at cooling down to the temperature of 0.45 K corresponding to the energy of Dzyaloshinskii-Moriya interaction.

II. EXPERIMENTAL DETAILS

Experiments were performed using a set of ESR spectrometers, combined with a superconducting 12 T solenoid and a ^{3}He cryostat, providing temperature down to 0.45 K. A standard of 2,2-diphenyl-1-picrylhydrazyl (known as DPPH) was employed as a $g = 2.00$ marker for the magnetic field. Backward wave oscillators, Gann diodes and klystrons were microwave sources, covering the range 0.5–250 GHz. The microwave units with cylindrical, rectangular, cut-ring, and spiral resonators were used for recording the resonance absorption of microwaves. In the case of a properly tuned resonator at frequency ν we observe the diminishing of the transmission, proportional to the imaginary part of the uniform susceptibility of the sample $\chi''(\nu,0)$. The ESR line of a conventional paramagnet, recorded in this case as a dependence of the transmission on the external field, should have a Lorentzian shape. Unfortunately, for frequencies above 200 GHz the spectrum of eigenfrequencies of the cavity is too dense and proper tuning is difficult; therefore, a distortion of the ESR line is possible. The presence of this parasitic effect was checked by recording test ESR lines at higher temperatures in the paramagnetic regime. In the case of a parasitic distortion an error for the resonance field of about a half of the resonance width was inserted.

The samples used in our measurements were the single crystals of $K_2CuSO_4Br_2$ from the same batch as in Ref. [15]. We used two samples with the principal structure axes matching the crystal facets. A smaller sample A had a mass of 6 mg, and a bigger sample B was about 64 mg. Sample B was used in experiments in lower frequency range $\nu < 25$ GHz, where larger size sample is required due to the larger resonator volume.

III. EXPERIMENTAL RESULTS

The temperature evolution of the 27.83 GHz ESR line is present in Fig. 3. Here the magnetic field is applied along the b axis, parallel to the DM vector **D**. We observe that a single ESR line with the g factor of 2.24 found in a paramagnetic phase at $T = 30$ K evolves at cooling in a spectrum of three components, labeled as M_+, M_-, and P. The components M_+ and M_- exhibit a shift from the paramagnetic resonance field, increasing with cooling. A weak line P remains at the paramagnetic resonance field. The temperature dependencies of the resonance fields of modes M_+ and M_-, as well as of mode P, are present in Fig. 4. The intensity of mode P grows with cooling following Curie law $1/T$; the linewidth also increases (see Fig. 5). Due to broadening this line is not so well visible at most low temperature, as for $T \simeq 4$ K.

One can see that the shift of resonance lines M_+ and M_- from the paramagnetic resonance field evolves with the decrease of temperature and saturates only around 1 K. These data expand the temperature range of previous measurements [15] to lower temperatures and reveal a saturation of the resonant field shift. The linewidth of mode P increases

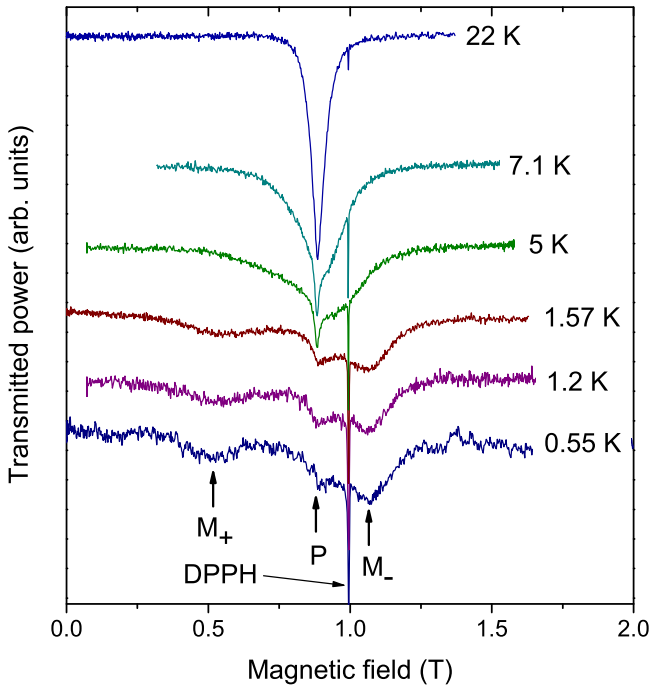

FIG. 3. (Color online) Temperature evolution of the 27.83 GHz ESR line of sample A at $\mathbf{H} \parallel b$. M_+ and M_- label the components of the doublet; P is a paramagnetic line associated with residual defects. A narrow line at 0.994 T is the DPPH label.

with cooling similar to the increase of the resonant field shift for modes M_-, M_+. It also saturates at $T \simeq 1$ K.

The temperature evolution of 27.75 GHz ESR spectrum at $\mathbf{H} \parallel a$ is present in Fig. 6. Here the single line $M_\pm$ survives at

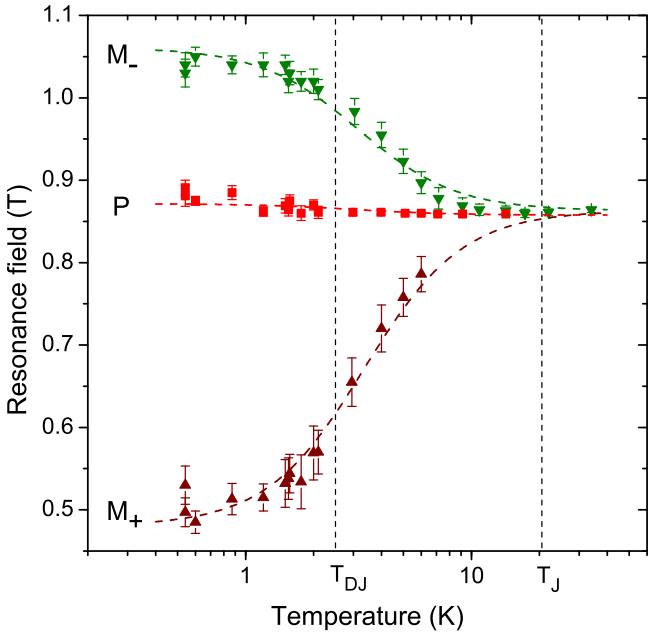

FIG. 4. (Color online) Temperature dependence of 27.83 GHz ESR fields at $\mathbf{H} \parallel b$ for the components of the doublet M_+, M_- and of the paramagnetic line P, associated with the defects. Characteristic temperatures marked on the horizontal axis are $T_{DJ} = \sqrt{DJ}/k_B$ and $T_J = J/k_B$. Dashed lines are guide to the eyes.

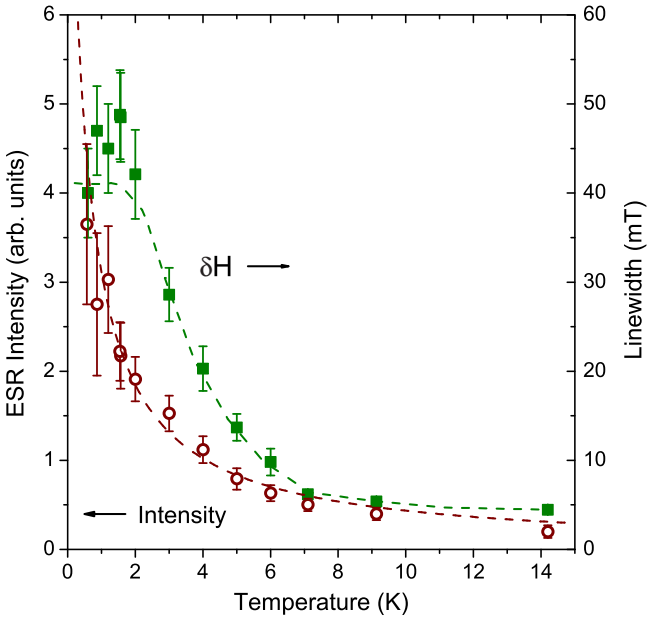

FIG. 5. (Color online) Temperature dependence of integral intensity (circles) and linewidth (squares, half width at half height) of mode P at $\nu = 27.83$ GHz. Dashed line passing near squares is a guide to the eyes; passing near circles is a $1/T$ Curie-law fit.

cooling, but demonstrates a shift to lower fields. The shift of this single mode also reaches a limit value at $T \simeq 1$ K as shown in Fig. 7. The transformation of the single-mode spectrum at $\mathbf{H} \parallel a$ into a doublet at $\mathbf{H} \parallel b$ is traced in the angular dependencies shown in Fig. 8. For the rotation of the magnetic field within the ac plane the single-mode spectrum is conserved and has a negligible angular dependence, as seen in the right panels of Fig. 8. The high-temperature ($T = 30$ K) g factors at these orientations $g_a \simeq g_c = 2.05 \pm 0.01$ are also identical.

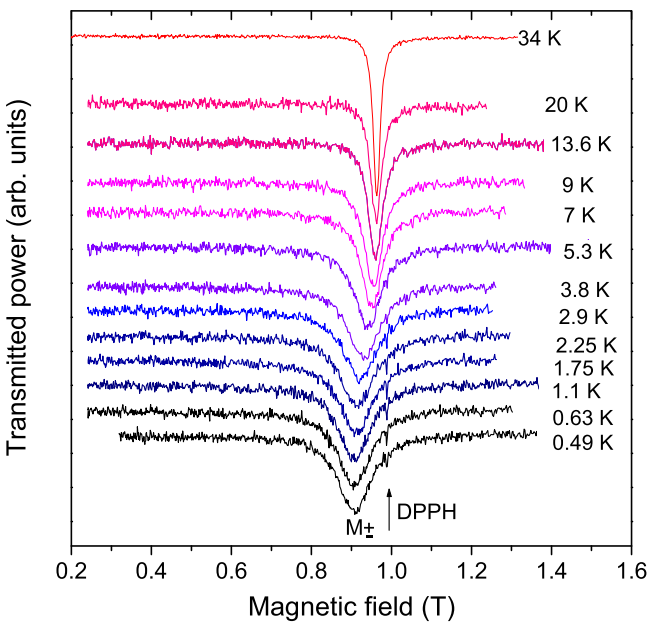

FIG. 6. (Color online) Temperature evolution of ESR line at frequency $\nu = 27.75$ GHz, $\mathbf{H} \parallel a$.

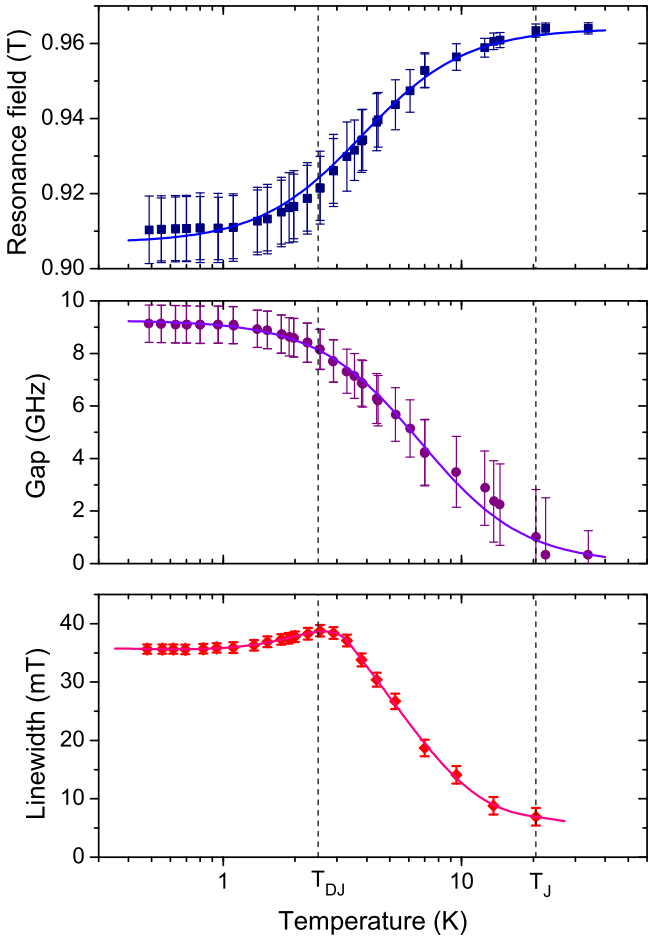

FIG. 7. (Color online) Upper panel: temperature dependence of 27.75 GHz ESR field at $\mathbf{H} \parallel a$. Middle panel: temperature dependence of the energy gap derived from the resonance field by means of relation (4). Lower panel: temperature dependence of 27.75 GHz ESR linewidth at $\mathbf{H} \parallel a$. Characteristic temperatures marked on the horizontal axis are $T_{DJ} = \sqrt{DJ}/k_B$ and $T_J = J/k_B$. Solid lines are a guide to the eye.

Examples of ESR records taken at different frequencies for $\mathbf{H} \parallel a,b$ are presented in Figs. 9, 10, and 11. The data for $\nu > 25$ GHz at $T \simeq 0.5$ K were taken using the sample A. For lower frequencies, for the reason described in Sec. II, we used sample B, which was studied at temperatures $T \gtrsim 1.3$ K. As the positions of resonance fields practically do not evolve below 1.3 K, the 1.3 K data present the low-temperature limit values of the resonance fields. Sample B has a larger relative intensity of impurity mode (P^* in Fig. 11) with respect to the intrinsic signal. The fraction of paramagnetic defects was estimated from the comparison of the total intensity of ESR signal in the paramagnetic phase ($T > 20$ K), with the intensity of defect ESR measured at $T \simeq 5$ K. Intensity of the paramagnetic signal at $T > 20$ K is ascribed to the total number of spins. The intensities of these two signals were measured at different temperatures. Therefore, we have normalized them to get the ratio of numbers of spins using the Curie-Weiss law with Curie-Weiss temperature $\theta = J/k_B$ for the main signal at $k_B T > J$ and Curie-Weiss law with $\theta = 0$

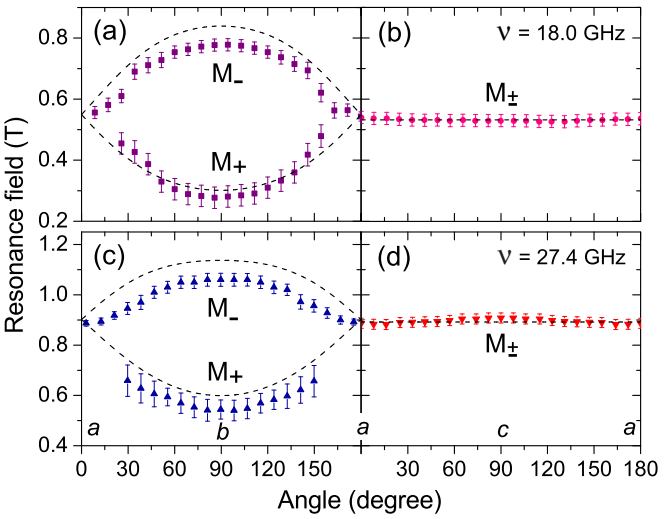

FIG. 8. (Color online) Angular dependencies of the resonant fields at two frequencies for $T = 1.3$ K. 18.0 GHz ESR fields for field in ab plane (upper left panel), and in ac plane (upper right panel). 27.4 GHz ESR fields for field in ab plane (lower left panel), and in ac plane (lower right panel). Dashed lines are theoretical dependencies according to (2).

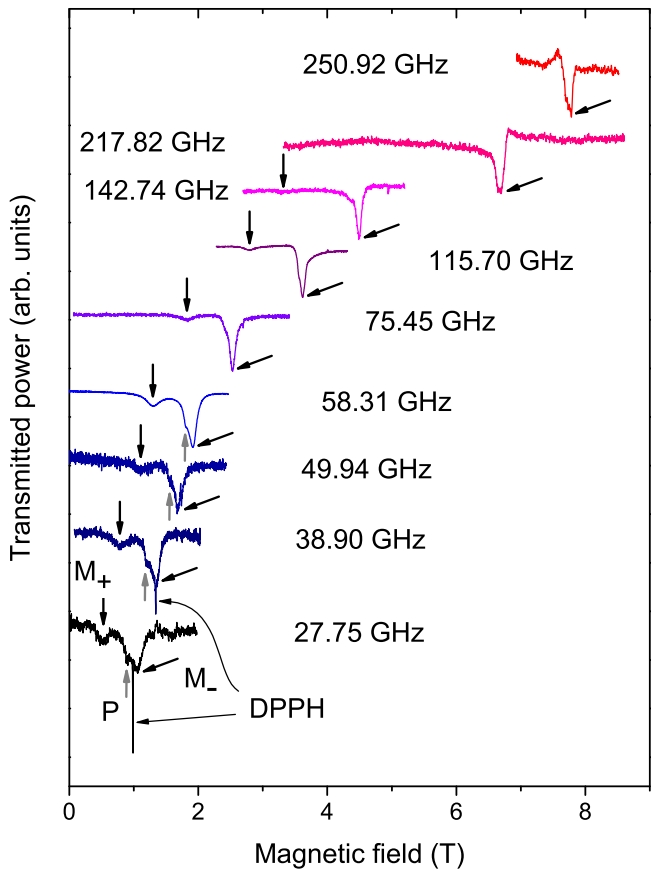

FIG. 9. (Color online) Examples of ESR lines at $\mathbf{H} \parallel b$ for $\nu > 25$ GHz, $T = 0.5$ K, sample A. Black arrows directed down mark mode M_+, tilted arrows—mode M_-. Gray arrows directed up mark paramagnetic mode P.

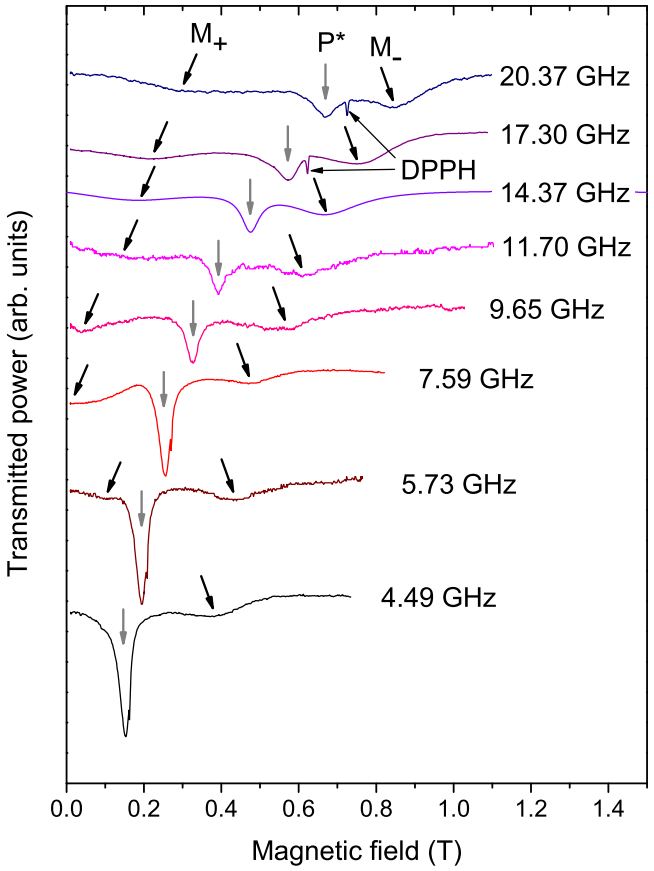

FIG. 10. (Color online) Examples of ESR lines at $\mathbf{H} \parallel b$ for the low frequency range $\nu < 25$ GHz, $T = 1.3$ K, sample B. Right and left tilted black arrows mark modes M_+ and M_- correspondingly. Vertical gray arrows mark paramagnetic mode P^*.

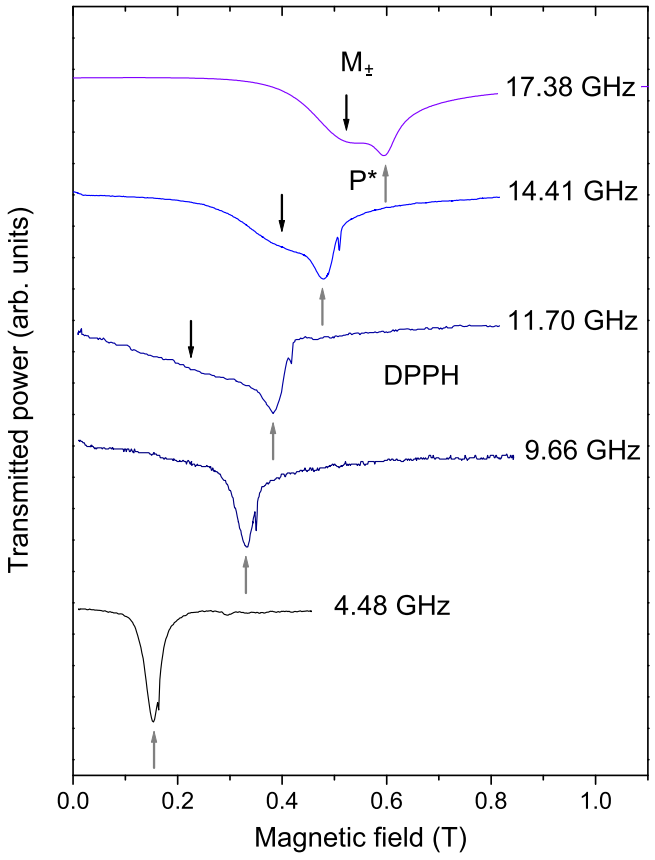

FIG. 11. (Color online) Examples of ESR lines at $\mathbf{H} \parallel a$ for different frequencies at $T = 1.3$ K, sample B. Black arrows indicate mode $M_\pm$; gray arrows mark paramagnetic mode P^*.

for ESR of defects. As a result, for sample A the content of defects was estimated as $x_A \simeq 0.008$, for sample B $x_B \simeq 0.02$.

Measurements of resonance fields of the intrinsic signal at different frequencies are summarized in frequency-field diagrams in Figs. 12 and 13. The formation of the zero-field gap of about 10 GHz is clearly seen here. Besides, for $\mathbf{H} \parallel b$ we see the falling branch, reaching zero frequency at $H_0 = 0.25$ T and a rising branch, originating from zero frequency at the same field. The latter transforms into the component M_- of the doublet in the frequency range above the gap. With the increase of the field the low-field component of the doublet vanishes and above 3.5 T we observe only a single line in the spectrum.

For $\mathbf{H} \parallel a$ and $\mathbf{H} \parallel c$ we observe in the whole field range only a single line (mode $M_\pm$ in Fig. 11) originating approximately at 10 GHz and a paramagnetic line of defects P^*, which has different intensity for different samples. At frequencies lower than 10 GHz we observe only the paramagnetic ESR line of defects.

The low-intensity residual paramagnetic line P correlates with the main ESR signal. At first, the broadening of mode P at cooling below 4 K has a temperature dependence analogous to that of the resonance field shifts for modes M_+, M_-, and $M_\pm$. The second evidence for correlation may be found in the angular dependence of ESR response taken at $T = 4.2$ K, which is present in Fig. 14. Here we see a narrow paramagnetic resonance line with $g \simeq 2.24$ at $\mathbf{H} \parallel b$. With the rotation of the magnetic field towards the a axis this narrow line shifts towards M_- and then merges with the main signal. As a result, at $\mathbf{H} \parallel a$ there is a single line with $g \simeq 2.10$. If the narrow line P would have survived as an independent signal, it would be seen as a narrow sharp peak on the background of a wider resonance line.

IV. DISCUSSION

A. ESR modes of a spin chain

The spinon continuum and the related ESR doublet observed in $K_2CuSO_4Br_2$ are consequences of quantum fluctuations in quasi-1D spin $S = 1/2$ system, which remains disordered far below the Curie-Weiss temperature. The observed formation of the ESR doublet M_+, M_- in the temperature range below the temperature $T_J = J/k_B$ is fully consistent with the scenario of the spin chain entering a quantum critical regime upon cooling. The anisotropic behavior of the doublet is in a perfect agreement with the symmetry considerations for Dzyaloshinskii-Moriya vector $\mathbf{D}$. The symmetry of the orthorhombic $Z = 4$ $Pnma$ structure of $K_2CuSO_4Br_2$ implies $\mathbf{D} \parallel b$, as shown in Fig. 1. The theory prediction (Refs. [9,10]) is that the ESR doublet should be observable only when the magnetic field has a component along $\mathbf{D}$. In a full

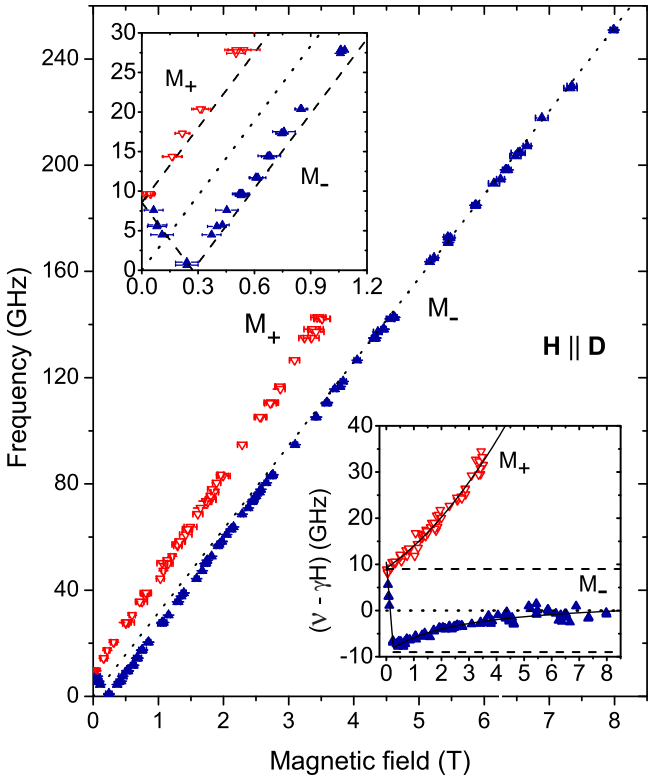

FIG. 12. (Color online) Main panel: frequency-field diagram for $\mathbf{H} \parallel \mathbf{D}$ at $T = 0.5$ K. Dotted line presents the Larmor frequency ν_0 (5). Upper inset: low-frequency part of the frequency-field diagram. Dashed lines present the theoretical prediction (3) for $D = 0.27$ K. Lower inset: resonance shift from the paramagnetic frequency for $\mathbf{H} \parallel b$ at $T = 0.5$ K. Dashed lines are drawn according to the theoretical prediction (3) for $D = 0.27$ K; dotted line marks zero offset from the paramagnetic resonance. Solid lines are a guide to the eye.

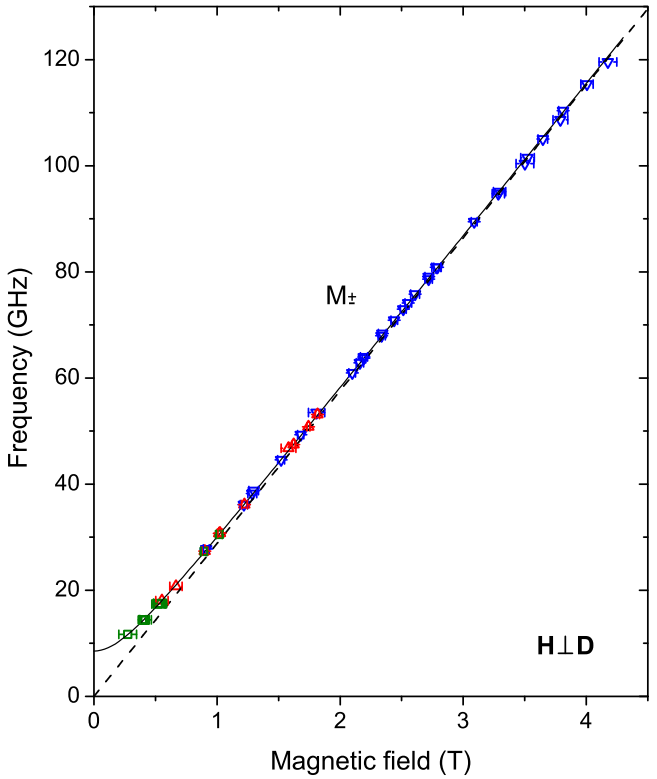

FIG. 13. (Color online) Frequency-field diagram for $\mathbf{H} \perp \mathbf{D}$ in the low-temperature limit. Data presented by ▽ correspond to sample A at $\mathbf{H} \parallel a$ and are taken at $T = 0.5$ K, △ present sample B at $T = 1.3$ K for $\mathbf{H} \parallel c$, and □ denote resonance field for sample B at $T = 1.3$ K and $\mathbf{H} \parallel c$. Solid line presents the theory (4) with parameters $D = 0.27$ K, $g_{ac} = 2.06$. Dashed line corresponds to ESR of the paramagnetic phase (5) at $T > 30$ K.

correspondence with the above symmetry restrictions we observe a doublet at $\mathbf{H} \parallel b$ and a single line at $\mathbf{H} \perp b$. For an arbitrarily aligned magnetic field $\mathbf{H} = (H_a, H_b, H_c)$ and $\mathbf{D} \parallel b$ the theoretical analysis [10] predicts the two following resonance frequencies:

$$(2\pi\hbar\nu_+)^2 = (g_a\mu_B H_a)^2 + (g_b\mu_B H_b + \pi D/2)^2 + (g_c\mu_B H_c)^2,$$
$$(2\pi\hbar\nu_-)^2 = (g_a\mu_B H_a)^2 + (g_b\mu_B H_b - \pi D/2)^2 + (g_c\mu_B H_c)^2. \quad (2)$$

In the limiting cases of $\mathbf{H} \parallel \mathbf{D}$ and $\mathbf{H} \perp \mathbf{D}$ the equation set (2) correspondingly transforms into

$$2\pi\hbar\nu_\pm = \left| g_b\mu_B H \pm \frac{\pi D}{2} \right|, \quad (3)$$

$$2\pi\hbar\nu_\pm = \sqrt{(g_\perp\mu_B H)^2 + \left(\frac{\pi D}{2}\right)^2}. \quad (4)$$

Here $g_\perp$ is the value of g factor for the field oriented perpendicular to b. These relations give the zero-field gap $2\pi\hbar\Delta = \pi D/2$ and the soft mode for $\mathbf{H} \parallel \mathbf{D}$ is predicted to occur at $H_0 = \pi D/(2g_b\mu_B)$.

B. Data analysis

In the above description of the low-temperature spectrum D is the *only* open parameter, as the g-factor values are given by the paramagnetic resonance at high temperatures (when $k_B T \gtrsim J$). This single parameter is easily determined from the zero-field energy gap Δ. We derive $\Delta = 8.7$ GHz by fitting the experimental $\nu(H)$ dependence for $\mathbf{H} \parallel a$ (Fig. 13) with the relation (4). Thus we get the value of $D = 0.27 \pm 0.015$ K. The frequency-field dependencies calculated for $\mathbf{H} \parallel b$ according to Eq. (3) are shown in the upper and lower insets of Fig. 12 by dashed lines. Both rising and falling branches, as well as a change from falling to rising behavior at $H_0 = 0.25$ T are in a good agreement with the theoretical predictions in the low-field regime at $H < 1.2$ T. We would like to note that observation of such a soft mode at H_0 is impossible in the other model compound Cs_2CuCl_4 due to noncollinear arrangement of DM vectors in adjacent chains. The low-frequency angular dependence of the ESR fields, taken at the rotation of the magnetic field in ab and ac planes is also in a good agreement with the theoretical relations (2), as shown in the upper panel of Fig. 8.

Nevertheless, the agreement gets worse with the field increase. Positions of the doublet components start to deviate from the calculated frequencies. One can see this behavior in

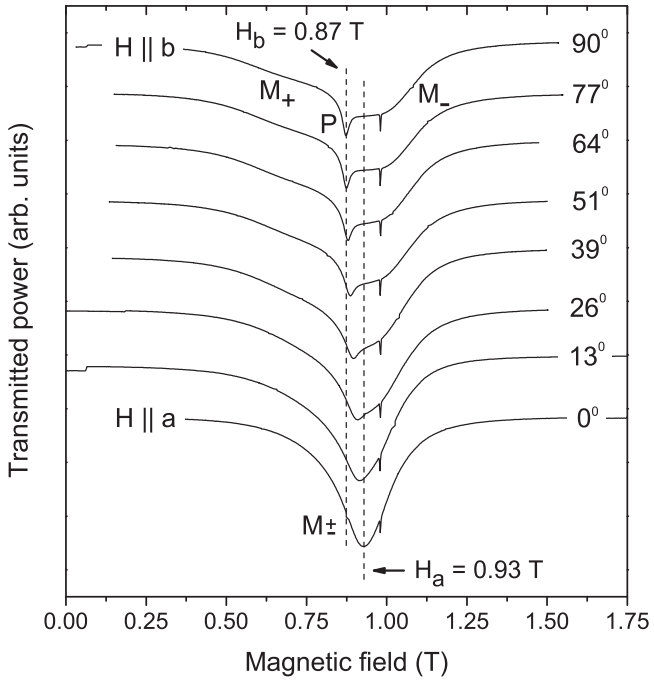

FIG. 14. Evolution of $\nu = 27.44$ GHZ ESR record with the magnetic field rotation in ab plane. Sharp resonance line at $H = 0.98$ T is the DPPH label with $g = 2.0$.

frequency-field diagrams of Fig. 12 as well as in $\nu \simeq 27$ GHz angular dependence in the lower panel of Fig. 8. The resonance shift of the component M_+ rises in a nonlinear way with the increasing field, while for the component M_- it gradually disappears. This behavior is emphasized in the "resonance shift" representation shown in the lower inset of Fig. 12. As the mode M_+ vanishes around 4 T, even a qualitative agreement with the theory predictions is completely lost. The spectrum becomes indistinguishable from a conventional paramagnet—a single line at Larmor frequency:

$$2\pi\hbar\nu_0 = g_b\mu_B H. \tag{5}$$

For $\mathbf{H} \perp \mathbf{D}$ the resonance at such high frequencies becomes indistinguishable from a paramagnetic spectrum as well, being, nevertheless, in accordance with theoretical relation (4).

On the one hand, this transformation to the Larmor-type ESR spectrum is not unexpected as the magnetic field suppresses quantum fluctuations which are the natural ground for the spinon continuum, and hence for the spinon ESR doublet. The theoretical analysis of the spinon continuum in a magnetic field predicts a collapse of the continuum at the saturation field [4]. The loss of the spectral density at the upper boundary of the continuum was predicted in a strong magnetic field in Ref. [16]. This should result in the deminishing of the M^+ mode intensity for the chain with the uniform DM interaction. On the other hand, the actual observed field of the doublet collapse is only 3.5 T, constituting about $0.13H_{\rm sat}$ (the saturation field of $K_2CuSO_4Br_2$ is about 27 T [15]). Such a low value of the collapse field indicates, probably, that the corresponding energy scale is related to *weak* DM interaction. One can empirically estimate the collapse field as $\sqrt{H_{\rm sat}D/(g\mu_B)} \simeq \sqrt{2DJ}/(g\mu_B) \simeq 3$ T. For the previously studied material Cs_2CuCl_4 the doublet collapse was observed at the magnetic field of about 4 T [14], which is a half of the saturation field. However, the DM interaction strength in this compound is larger, corresponding to zero-field ESR gap of 14 GHz. The estimation according to the above empiric rule gives 4 T for Cs_2CuCl_4 in a good agreement with the experiment. It is worth noting that the final formation of the doublet and the maximum of the resonance field shift for the doublet components in $K_2CuSO_4Br_2$ are achieved at $T^* \simeq 1$ K, which is much lower than the characteristic exchange temperature $J/k_B \simeq 20$ K. The value of T^*, analogous to the field of the doublet collapse is rather of the order of intermediate temperature $T_{DJ} = \sqrt{DJ}/k_B$ than of the order of the exchange temperature T_J.

C. Paramagnetic defects

The paramagnetic mode P observed at $\mathbf{H} \parallel b$ in sample A may be separated from the ESR signal of the main matrix in the temperature interval $1.3 < T < 14$ K due to its narrow line and the position, different from the resonances M_- and M_+ (see Fig. 3). The position of line P does not depend on temperature and corresponds to the g-factor value g_b of the paramagnetic phase within the experimental accuracy. This indicates that the mode P may originate from intrinsic defects such as breaks of the spin chains. The growth of the linewidth of signal P at cooling is similar to the growth of the energy gap Δ and the mode $M_\pm$ linewidth, as shown in Fig. 7. This observation confirms the proposition on the interaction between the defects and the spin chains.

The growth of the linewidth may be qualitatively explained by the proposition of an effective exchange interaction between the defects and spinons. Further, we consider the linewidth using a concept of the exchange narrowing and broadening developed by Anderson [17]. Indeed, the exchange interaction J^* between two magnetic systems with the resonance frequencies differing for $\delta\omega$ is known to modify the ESR spectrum. In the case of the "slow" exchange ($J^*/\hbar < \delta\omega$), the lines of the initial spectrum are broadened, while at $\delta\omega = 0$ the broadening is absent. This may presumably explain the broadening of the mode P at cooling as the difference in resonance frequencies of modes M_-, M_+ and mode P develops. This implies a value of J^* of about or less than the difference between the energies of modes $M_\pm$ and P, i.e., 0.25 K. This value is naturally much smaller than the main exchange integral J, because spinons are delocalized within a chain. In the case of a "fast" exchange ($J^*/\hbar > \delta\omega$) the ESR lines should merge into a single narrow line [17]. The vanishing of the defect mode P at the rotation of the magnetic field in the ab plane, present in Fig. 14, may be attributed to the transition from the slow exchange at $\mathbf{H} \parallel b$ (lines are observed separately) to the fast exchange at $\mathbf{H} \parallel a$, when the difference between resonance frequencies becomes smaller because of the angular dependence and the lines may merge due to the effective exchange J^*. In the absence of interaction between the defects and spin-chain matrix the narrow line P should be observable together with the wider line M_-.

V. CONCLUSION

A detailed ESR study of the quasi-1D $S = 1/2$ antiferromagnetic system with uniform Dzyaloshinskii-Moriya

interaction was performed. The energy gap of 8.7 GHz was observed in zero field and a characteristic doublet of resonance lines was found in a magnetic field. The zero-field gap, ESR doublet, and its anisotropy, as well as the frequency-field dependencies for three orientations of the magnetic field, are in a good agreement with the theory of spinon continuum modification by uniform Dzyaloshinskii-Moriya interaction, compatible with crystal symmetry of $K_2CuSO_4Br_2$. There is only one fitting parameter in this theory. On the other hand, with the increase of the magnetic field the low-frequency approximation fails, and the deviation from the linear frequency-field dependencies in a high field and vanishing of the doublet in a rather low field of $0.13H_{\rm sat}$ are not understood now. The system of magnetic defects, interacting with the spin excitation of the main matrix was also revealed by ESR experiment.

ACKNOWLEDGMENTS

We thank V. N. Glazkov, S. S. Sosin, and L. E. Svistov for numerous discussions and comments, and for help with microwave spectrometers, and O. A. Starykh for discussions. Work at the Kapitza Institute is supported by Russian Foundation for Basic Research, Grant No. 15-02-05918, and by the Program for Basic Research of the Presidium of Russian Academy of Sciences. ETHZ team acknowledges support from Swiss National Science Foundation, Division 2.

[1] L. D. Faddeev and L. A. Takhtajan, What is the spin of a spin wave?, Phys. Lett. A **85**, 375 (1981).

[2] D. A. Tennant, R. A. Cowley, S. E. Nagler, and A. M. Tsvelik, Measurement of the spin-excitation continuum in one-dimensional $KCuF_3$ using neutron scattering, Phys. Rev. B **52**, 13368 (1995).

[3] B. Lake, D. A. Tennant, J.-S. Caux, T. Barthel, U. Schollwöck, S. E. Nagler, and C. D. Frost, Multispinon Continua at Zero and Finite Temperature in a Near-Ideal Heisenberg Chain, Phys. Rev. Lett. **111**, 137205 (2013).

[4] G. Müller, H. Thomas, H. Beck, and J. C. Bonner, Quantum spin dynamics of the antiferromagnetic linear chain in zero and nonzero magnetic field, Phys. Rev. B **24**, 1429 (1981).

[5] D. C. Dender, P. R. Hammar, Daniel H. Reich, C. Broholm, and G. Aeppli, Direct Observation of Field-Induced Incommensurate Fluctuations in a One-Dimensional $S = 1/2$ Antiferromagnet, Phys. Rev. Lett. **79**, 1750 (1997).

[6] M. Oshikawa and I. Affleck, Electron spin resonance in $S = \frac{1}{2}$ antiferromagnetic chains, Phys. Rev. B **65**, 134410 (2002).

[7] I. Dzyaloshinsky, A thermodynamic theory of "weak" ferromagnetism of antiferromagnetics, J. Phys. Chem. Solids **4**, 241 (1958).

[8] T. Moriya, Anisotropic superexchange interaction and weak ferromagnetism, Phys. Rev. **120**, 91 (1960).

[9] S. Gangadharaiah, J. Sun, and O. A. Starykh, Spin-orbital effects in magnetized quantum wires and spin chains, Phys. Rev. B **78**, 054436 (2008).

[10] K. Yu. Povarov, A. I. Smirnov, O. A. Starykh, S. V. Petrov, and A. Ya. Shapiro, Modes of Magnetic Resonance in the Spin-Liquid Phase of Cs_2CuCl_4, Phys. Rev. Lett. **107**, 037204 (2011).

[11] H. Karimi and I. Affleck, Transverse spectral functions and Dzyaloshinskii-Moriya interactions in XXZ spin chains, Phys. Rev. B **84**, 174420 (2011).

[12] Y. Ajiro, ESR experiments on quantum spin systems, J. Phys. Soc. Jpn. **72**, 12 (2003).

[13] A. I. Smirnov, K. Yu. Povarov, S. V. Petrov, and A. Ya. Shapiro, Magnetic resonance in the ordered phases of the two-dimensional frustrated quantum magnet Cs_2CuCl_4, Phys. Rev. B **85**, 184423 (2012).

[14] A. I. Smirnov, T. A. Soldatov, K. Yu. Povarov, and A. Ya. Shapiro, High-field magnetic resonance of spinons and magnons in a triangular lattice $S = 1/2$ antiferromagnet Cs_2CuCl_4, Phys. Rev. B **91**, 174412 (2015).

[15] M. Hälg, W. E. A. Lorenz, K. Yu. Povarov, M. Månsson, Y. Skourski, and A. Zheludev, Quantum spin chains with frustration due to Dzyaloshinskii-Moriya interactions, Phys. Rev. B **90**, 174413 (2014).

[16] M. Kohno, Dynamically Dominant Excitations of String Solutions in the Spin-1/2 Antiferromagnetic Heisenberg Chain in a Magnetic Field, Phys. Rev. Lett. **102**, 037203 (2009).

[17] P. W. Anderson, A mathematical model for the narrowing of spectral lines by exchange or motion, J. Phys. Soc. Jpn. **9**, 316 (1954).